Contents lists available at GrowingScience

Engineering Solid Mechanics

homepage: www.GrowingScience.com/esm

The effect of stacking sequence and fiber orientation on tensile and flexural strength of fiber reinforced composite fabricated by VARTM process

Himanshu V. Patel[a] and Harshit K. Dave[a*]

[a]*Sardar Vallabhbhai National Institute of Technology, Ichchhanath Surat, India*

A R T I C L E I N F O

Article history:
Received 24 January 2022
Accepted 1 September 2022
Available online
1 September 2022

Keywords:
Vacuum Assisted Resin Transfer Molding
Tensile strength
Flexural strength composite
Stacking sequence
Fiber orientation
Fiber reinforced composite

A B S T R A C T

In this study, Carbon, Glass, and Aramid fiber reinforced composite and their hybridized forms were fabricated using five different stacking sequences of the fabrics. Using the Vacuum Assisted Resin Transfer Molding (VARTM) procedure, epoxy resin was injected into these fabrics and allowed to cure at room temperature. From these five stacking sequences, a standard specimen with four different orientations viz. 0/90°, 15/75°, 30/60°, 45/-45° orientations were obtained using the Abrasive Water Jet Machining(AWJM) Process. The influence of stacking order and fiber orientation on tensile and flexural properties of composite was investigated. From the result of tensile testing, the highest and lowest tensile strength values were observed for neat carbon fiber reinforced composite at 0/90° orientation and at 45/-45° orientation respectively. The highest flexural strength was achieved in a hybrid combination of two layers of carbon, glass and aramid fabric for 0/90° whereas the lowest flexural strength was found in glass reinforced composite for the 45/-45° orientation.

1. Introduction

Fiber Reinforced Composites (FRCs) are used as key constructions for aerospace vehicles, launch vehicles/space vessels for space travel and in the field of sports. Polymer matrix composites provide high strength and lightweight at the same time for the structural components. The major reasons for adopting FRPC are the lightweight design capability, the flexible deformation behavior, high corrosion resistance, and low electrical conductivity depending on the fiber composition. (Song, 2016). The hybrid composite material can be achieved using intrayarn, intralayer and interlayer configurations. Due to the fact that hybrid composites contain many reinforcing elements in a single matrix, it is crucial to maximise the synergistic effects of these reinforcements' characteristics on the composites' overall characteristics (Swolfs et al., 2019). Man-made or natural reinforcement materials can be used to develop hybrid composite components. These hybrid composite components offer better mechanical properties with lightweight so they fulfill the demand of automotive, aerospace and sports goods manufacturing industries (Bindal et al., 2013; Murugan et al., 2014) For manufacturing of advanced composite, Resin Transfer Molding (RTM) is one of the cost-effective methods in which simpler tools are used.The RTM method is consist of applying a layer of strands, braided fibers or performs to a mold and then resin is injecting and curing. For the quality products RTM and its variations such as vacuum-assisted resin transfer molding (VARTM), Resin Infusion under Flexible Tooling (RIFT), and Seemann Composites Resin Infusion Molding Process (SCRIMP) are widely used (Naik et al., 2014; Simacek et al., 2012). Teixeira and Souza (2019) performed a numerical simulation to determine the advancement of resin flow inside the mold cavity of the small vessel hull. They identified the ideal placement for injection tubes and the start time for resin injection. They found that from the study correct resin injection time at inlet or vent can be helpful to reduce air bubbles. Golzar and Poorzeinolabedin (2010) designed and fabricated a body cover prototype using E-glass/epoxy. The fabrication of the body cover prototype was done by vacuum bagging process. They found that 42% weight reduction with higher mechanical performance compared to steel cover. Bhagat et al., (2014) fabricated hybrid reinforced polymer matrix composite using glass

* Corresponding author.
E-mail addresses: harshitkumar@yahoo.com (H. K. Dave)

ISSN 2291-8752 (Online) - ISSN 2291-8744 (Print)

doi: 10.5267/j.esm.2022.9.001

fibers and coir fibers. They concluded that fiber loading and fiber length affects the characteristics of composite viz. density, hardness, tensile and flexural properties. The highest tensile and flexural strength was achieved in 10 % of fiber weight loading at 15 mm length. Dippenaar and Schreve (2013) investigated rapid tooling for VARTM using 3D printing. This 3D printed mold was used for making blades for turbines. From the investigation, they concluded that 3D printed tooling is more beneficial for VARTM process tooling in terms of processing time and cost-effectiveness compared to conventional tooling. Singh et al (2017) reported several improvements to the matrix and used glass fiber reinforcement to produce hybrid composite laminates. From their investigation they found that mechanical strength of the composite laminate is affected by the fiber volume fraction, fiber length, fiber orientation, alkali treatment, aging behavior under particular environment and water absorption properties.

Olodo et al., (2021) created a glass/polyester composite laminate. They tested this laminate through impact shock testing. They discovered that fracture energy is proportional to impact speed. The results were used for the construction of multilayer structures subjected to impact loads. The bending characteristics of woven carbon/glass and carbon/aramid fiber reinforced polymer composites were examined by Song (2014). Using VARTM, carbon/aramid and carbon/glass fabrics were laminated to create six distinct hybrid composite configurations. They concluded that the position of carbon fiber placement is having a crucial impact on the flexural strength of the composite structure. Islam et al. (2015) developed hybrid composite which was made up of carbon-kevlar hybrid composite and it suitable to store fuel tank of space vehicle. Sharafi et al. (2018) fabricated new and efficient sandwich panels for structural walls. They examined the flexural and shear behavior of these panels both experimentally and numerically. They noticed a good agreement between experiment and numerical simulation. Flynn et al. (2016) manufactured hybrid composite laminates using carbon fiber and flax fiber with varying flax fiber volume fractions. Seven specimens were fabricated using different stacking sequences. Tensile, impact and bending tests were conducted and it was reported that the mechanical characteristics of natural fibre composites can be successfully enhanced by combining synthetic and natural fibres.

Subagia and Kim (2013) fabricated hybrid composite with carbon and basalt fibers using VARTM process. They studied the influence of different stacking orders of carbon and basalt fiber plies on bending properties. They reported that among all stacking orders in which carbon fiber fabrics were at the most layer exhibit higher flexural strength compared to those with other reinforcement at the most layer. Dong and Davies (2015) studied the effect of volume fraction on the flexural performance of intralayer composite fabricated from glass fiber and carbon fiber reinforcement. They also simulated three levels of fiber volume fraction and four levels of span/depth ratio in the FEA model. It was observed that flexural strength increased with the span/depth ratio. Maximum flexural strength was achieved at 70% fiber volume fraction. Selver et al.,(2018) fabricated hybrid composite by varying stacking sequences using a glass, jute and flax fiber fabrics with resin infusion method and they tested specimens for tensile, flexural, and dynamic mechanical analyses (DMA) of the composite. They observed that the stacking sequence affects the flexural properties and DMA while there was no significant effect found on tensile strength. They also reported that composites fabrication using natural fibers is cost-effective and lightweight. Deng et al., (2015) prepared hybrid fiber Graphene Oxide / Carbon fiber using electrophoretic deposition process. They investigated surface morphologies and mechanical properties of the fabricated composite. From the result of the interlaminar shear strength test, they found significant improvement by introducing GO in Carbon reinforced composite. Umer et al., (2015) fabricated glass fiber composite using graphene oxide (GO)-modified epoxy resin system by VARTM process. They have studied rheological behavior and cured kinematics of the GO-modified resin system. They have also conducted a flexural test of fabricated parts. From the investigation, they concluded that the GO-based modified resin system has a faster curing rate and high viscosity compared to epoxy resin systems.

The better flexural strength was achieved using secondary filler at 0.2 wt% GO. Kaushik et al. (2017) manufactured a composite using polyester and epoxy as matrix material and jute as reinforcement material. They conducted flexural, impact, and erosion tests to explore characteristics. They discovered that Jute/epoxy composites performed better. An epoxy-based hybrid composite made of sisal, banana, and coir fibres was created by Balaji et al. (2019). They assessed the mechanical properties and water absorption of hybrid composites. The combination of sisal/epoxy composite among all laminates was observed to have the highest tensile and flexural strength. Sezgin and Berkalp (2017) produced hybrid composite using a combination of man-made and natural reinforcements. They have adopted a vacuum infusion process and developed several stacking sequences. They prepared specimens for impact and tensile testing by cutting along weft and warp directions. From the results, they determined that impact and tensile strength in the warp direction were larger as compared to weft direction. Bhudolia et al. (2018) manufactured thin hybrid composite laminates using carbon, Kevlar and glass fibers by RTM method. They manufactured three stacking sequences using these three fibers for vibration testing, bending testing, and impact testing. From their investigation, they concluded that bending strength increases with increment in the amount of Kevlar fibers.

Literature shows that hybrid composite can be fabricated using different man-made fibers, natural fibers or a combination of both. However, very little literature is observed to the best of authors' knowledge that reports the influence of fiber orientation and stacking sequence on tensile and flexural strength of composite laminates fabricated using VARTM process. In the present study, an attempt is made to study the influence of fiber orientation and stacking sequence on tensile and flexural strength of woven fabric reinforced hybrid composite. The paper also discusses damage assessment during tensile and flexural testing.

2. Plan and procedure

2.1 Materials

In present work, Carbon Fiber (CF), Glass Fiber (GF), and Aramid Fibers (AF) are used as reinforcement. The properties of all three fabrics are given in Table-1. These fabrics are plain woven having 0° and 90° weaving as seen in Fig. 1. Epoxy resin and Hardener are used as the matrix material and mixed in a ratio of 100:18 by weight to fabricate composite material as per the manufacturer data sheet.

Table 1
Properties of materials used

	CF	GF	AF
Areal weight (g/m^2)	200	105	220
Density (g/cm^3)	1.8	2.62	1.4
Fiber size (µm)	7	7	12
Tensile strength (MPa)	4000	3100	3097
Young's modulus (GPa)	240	80	105
Expansion (%)	1.7	4.8	2.8

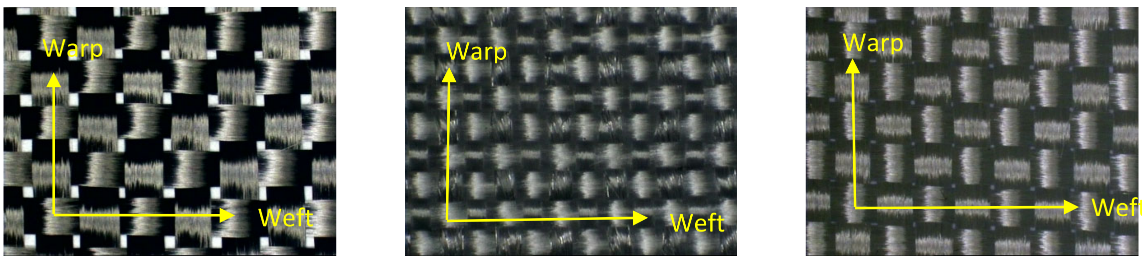

(a) CF Reinforcement **(b) GF Reinforcement** **(c) GF Reinforcement**
Fig. 1. Photograph of fiber fabric

2.2 Composite Fabrication

VARTM process was used for composite fabrication process was used to fabricate composite material using hybrid reinforcement fabrics and epoxy resin. A pictorial view of the VARTM process is shown in Fig. 2.

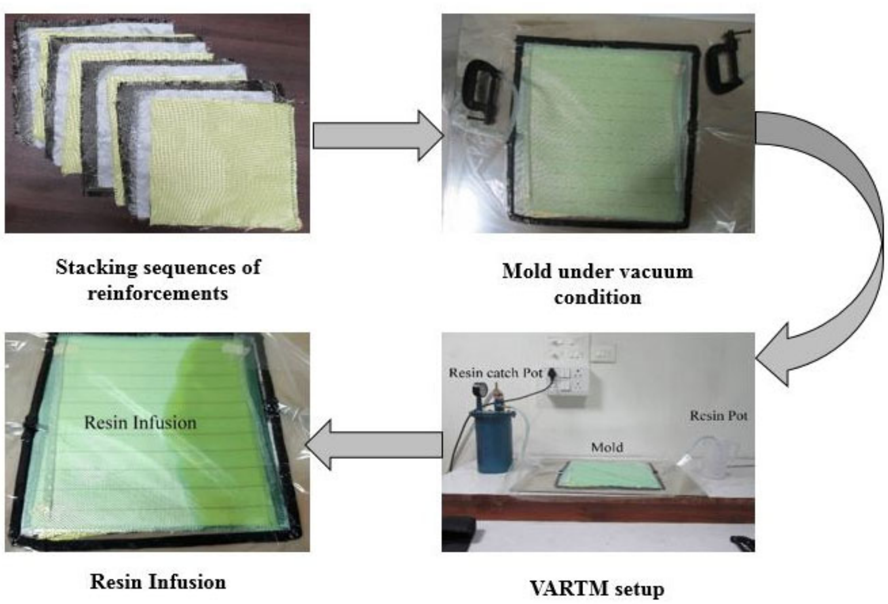

Fig. 2. Pictorial view of the VARTM Process

Reinforcement was cut in dimensions of 300 × 300 mm^2 and stacked in the mold. Peel ply was applied over the reinforcement materials which were used for demolding of the composite sheet after completion of the process. Over the peel ply, infusion mesh was applied which served as distribution media for the stacked reinforcement materials. After stacking, the entire mold was sealed with a flexible Vacuum bag using a sealant tape. Resin infusion was carried out at -1 bar pressure. And after full infusion, the sealed mold was kept for curing for 24 hours at room temperature. Demolding of the cured composite sheet was carried out manually after 24 hours and the specimen was prepared following ASTM standards of tensile and flexural testing. Using the twelve layers of fabrics total five different stacking sequences were obtained as listed in Table 2.

Table 2
Stacking sequences

Sr. No.	Sample Code	Stacking sequence	Stacking structure
		Neat Specimen	
1	R-1	C-12 (12 layers of CF)	CF_1- $CF_{2.}$ – …..CF_{12}
2	R-2	G12 (12 layers of GF)	GF_1- $GF_{2.}$ – ….GF_{12}
3	R-3	A12 (12 layers of AF)	AF_1- $AF_{2.}$ – ….AF_{12}
		Hybrid Specimen	
4	R-4	$(CGA)_4$ (Hybrid-1)	$CF_1GF_1AF_1$-….. $CF_1GF_1AF_1$-
5	R-5	$(C_2\ G_2\ A_2)_2$ (Hybrid-2)	$CF_2GF_2AF_2$- $CF_2GF_2AF_2$

Total five different combinations of stacking sequences were used for the composite laminated sheet as shown in Fig. 3.

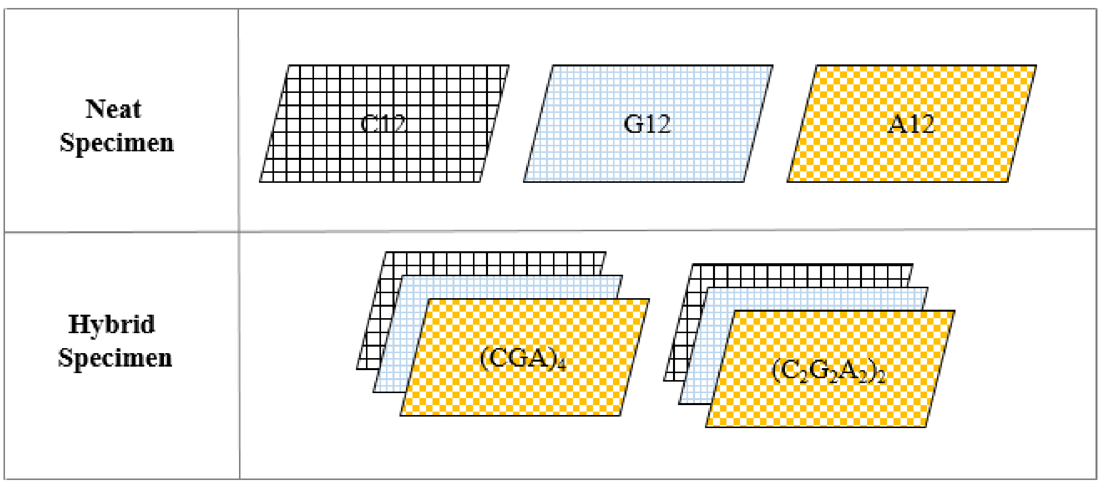

Fig. 3. Stacking sequence of composite laminates

2.3 Testing of Composite Laminates

From the aforementioned five combination layers illustrated in Fig. 3, four orientations viz. 0/90°, 15/75°, 30/60°, and 45/-45° were obtained. The orientations were measured along the weft and warp directions. These fiber oriented samples were cut using AWJM to prevent thermal deterioration and to create a smooth finish of the sample. Fig. 4 illustrates orientations which were achieved on plain weave reinforcement composite.

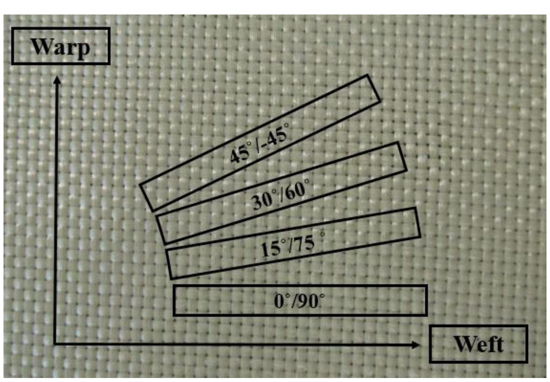

Fig. 4. Orientation of specimens which was cut on AWJM

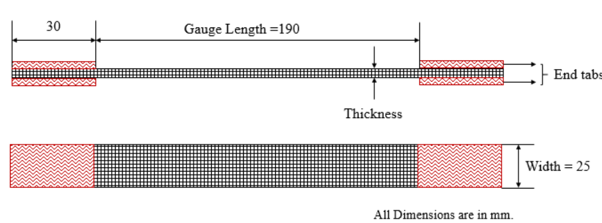

Fig. 5. Dimension of the tensile specimen

Tensile testing determines the behavior of the specimen when a pulling force acts on it under optimum conditions. Flexural testing measures the force required to bend a specimen. The flexural specimen is placed horizontally above two points of contact during flexural testing, and a force is then delivered to the top of the specimen through points of contact. For the tensile testing, the rectangle specimens were cut as per ASTM standard D3039. An emery cloth tab adhered at the end of the specimens using epoxy glue to avoid premature fracture of the specimens. The dimension of the tensile specimen was 25 mm × 250 mm × t mm where t was the actual thickness of the specimen. The dimension of the tensile specimen is shown in Fig. 5. The tensile strength of the fabricated composites was conducted using Instron 3382 universal testing machine (UTM) with crosshead speed 2 mm/min as shown in Fig. 6.

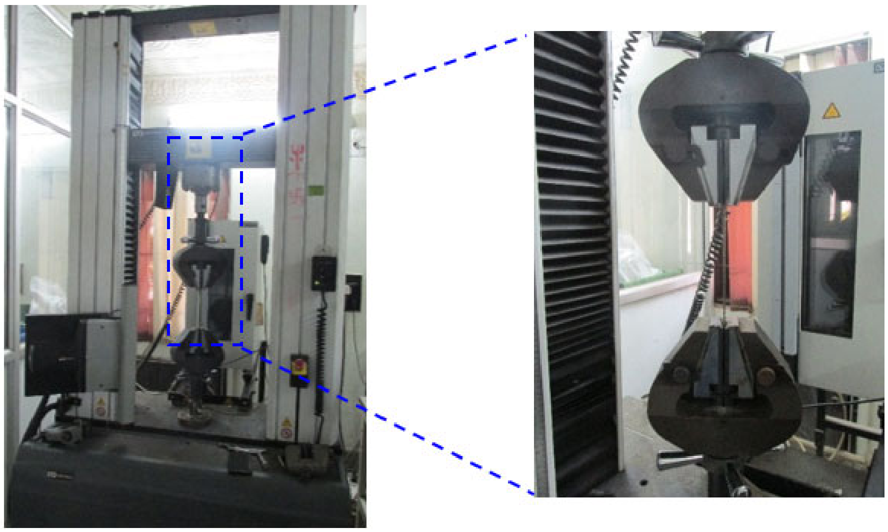

(a) Tensile testing machine **(b) Tensile specimen during testing**

Fig. 6. Tensile testing machine and specimen during tensile testing

The following equation was used to compute ultimate tensile strength.

$$\sigma_T = \frac{P_{max}}{A} \tag{1}$$

where, σ_T = ultimate tensile strength, Pmax = maximum force before failure, A= Average cross-sectional area.

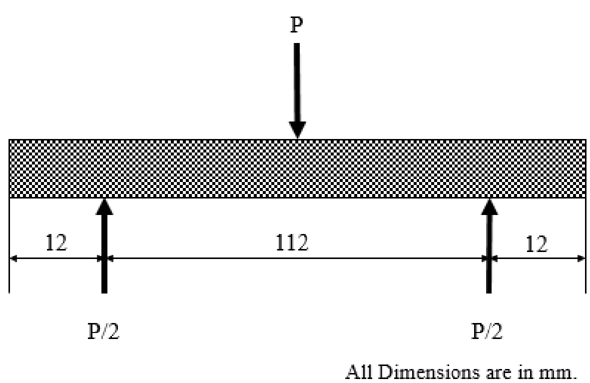

Fig. 7. Flexural specimen dimensions

The flexural specimens were prepared according to ASTM standard D7264. The length of the specimens was set to ensure the span/depth ratio of 32. Specimen preparation was done accordingly. The dimension of the flexural specimen was 13 mm × 136 mm × t mm, where t was the actual thickness of the specimen. The dimension of the flexural specimen as shown in Fig. 7. The flexural testing was done using Shimadzu AG-IS as shown in Fig. 8. The following equation was used to calculate the flexural strength:

$$\sigma_F = \left(\frac{3PL}{2bh^2} \right) \quad (2)$$

where, σ_F = stress at the outer surface at mid-span, P = applied force, L = support span, b = width of the specimen and h = thickness of the specimen.

The crosshead displacement rate was maintained at 1 mm/min. Span /depth ratio was chosen 32:1. Fig. 8 shows the flexural specimen during testing.

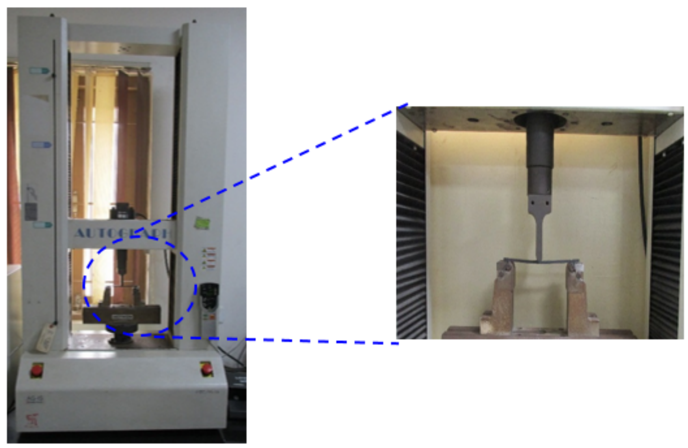

(a) Flexural testing machine **(b) Flexural specimen during testing**

Fig. 8. Flexural testing machine and specimen during flexural testing

The special properties of a hybrid composite material can be used to meet the design criteria for strength and flexural behaviour. A crucial component in the composite structure is the stacking order. The placement of the reinforcing places affects the mechanical characteristics of composite laminates. To check the effect of stacking sequence on composite laminates five fiber arrangements were taken. For each combination of stacking sequence and orientation, three test samples were used. The mean value of tensile as well as flexural strength was used for further study. These values are enlisted in Table-3.

Table 3. observed values of tensile testing and flexural testing

Sr. No.	**stacking sequence** S	**Orientation,** θ, Degree	**Mean Tensile Strength,** σ_t, (MPa)	**Standard Deviation,** S_T	**Mean Flexural Strength,** σ_f, (MPa)	**Standard Deviation,** S_F
1	C12	0/90	454.50	36.45	291.21	44.83
2	C12	15/75	203.03	3.43	215.87	34.59
3	C12	30/60	127.76	2.25	131.03	8.48
4	C12	45/-45	114.11	8.44	117.86	8.03
5	G12	0/90	66.74	11.24	81.05	9.88
6	G12	15/75	101.39	3.73	48.77	8.02
7	G12	30/60	87.38	15.20	31.34	4.32
8	G12	45/-45	85.37	5.86	31.05	1.26
9	A12	0/90	309.97	49.14	140.59	61.35
10	A12	15/75	147.60	15.20	121.80	7.74
11	A12	30/60	143.35	5.06	71.33	9.80
12	A12	45/-45	132.52	25.48	60.86	7.79
13	$(CGA)_4$	0/90	421.07	5.74	296.46	35.69
14	$(CGA)_4$	15/75	235.95	7.18	205.39	36.10
15	$(CGA)_4$	30/60	117.34	17.76	123.84	24.70
16	$(CGA)_4$	45/-45	120.58	25.87	70.02	8.46
17	$(C_2G_2A_2)_2$	0/90	298.48	31.83	362.79	39.12
18	$(C_2G_2A_2)_2$	15/75	179.75	24.26	212.69	12.81
19	$(C_2G_2A_2)_2$	30/60	161.90	2.13	119.15	5.83
20	$(C_2G_2A_2)_2$	45/-45	116.21	16.81	87.49	4.25

The total 60 samples each for a tensile and flexural specimen were tested for this study.

3. Result and Discussions

Table 3 presents the mean of the three observed data from the tensile and flexural testing of the fabricated specimen by varying stacking sequence and fiber orientation. For testing of the fabricated composite specimen, each configuration test was repeated three times.

3.1 Tensile Behavior

The Tensile behavior of the fiber reinforced polymer matrix composite was examined with a tensile test. The influence of stacking sequence and fiber orientation on tensile strength is discussed in subsequent sections.

3.1.1 Influence of stacking sequence on Tensile strength

Fig. 9 illustrates the tensile behavior of five different stacking sequences of composite laminates.

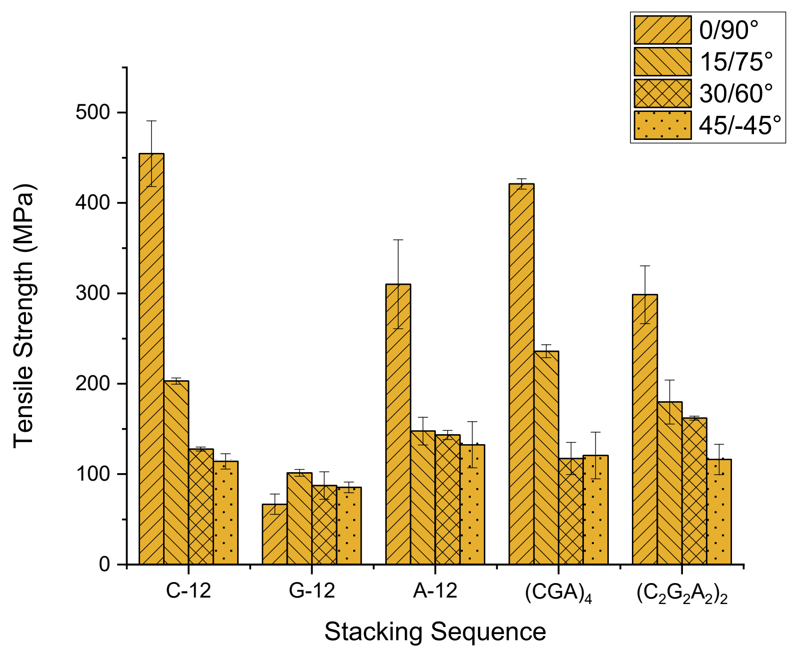

Fig. 9 Tensile strength vs stacking sequences

It can be observed that neat carbon fiber reinforced composite has the highest tensile strength among all five stacking sequences. Further, the lowest tensile strength was observed for neat glass fiber reinforced composite.The highest tensile strength was achieved in a stacking sequence having twelve carbon at orientation 0/90°. Loading direction and fiber direction for specimens at the orientation of 0/90° is the same during tensile testing of the specimen. During the tensile test of the laminate, the tensile force produces in the direction of the load, and the reinforcing fibers generate a reaction force against the tensile force. For 0/90° orientation, either the warp or weft fibers are in the direction of direct tensile load. Carbon reinforced composite is able to bear more load compared to other fiber reinforced material. So the tensile strength of the neat carbon reinforced composite specimen was found higher compared to other combinations of the specimen. To evaluate failure modes during tensile testing of all 0/90° samples, images were captured by Sipcon's make vision measurement equipment. Fig. 10 (a) shows a fractured cross-section of neat carbon reinforced composite which was held vertical by means of the binder clip. Identical pattern of fracture was observed during tensile testing of all composite laminates in the 0/90° direction as shown from Fig. 10 (a)-(e). The fracture patterns such as flat failure of the laminates and delamination of laminates were observed in all five stacking sequences at 0/90° orientation. Fiber rupture and fiber pullout were noticed in warp direction whereas fibers in weft direction remain undeformed. The delamination and flat breakage were also seen in the loading direction.

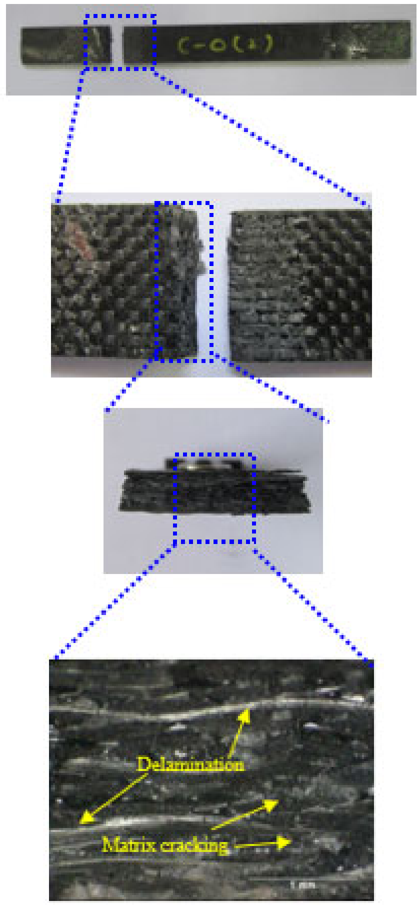

(a) C-12 at 0/90°

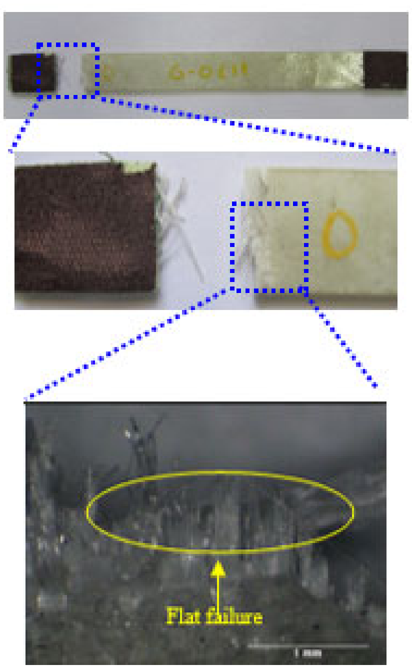

(b) G-12 at 0/90°

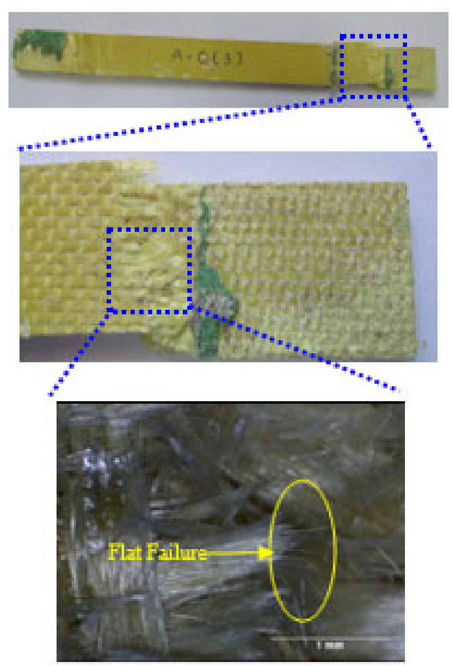

(c) A-12 at 0/90°

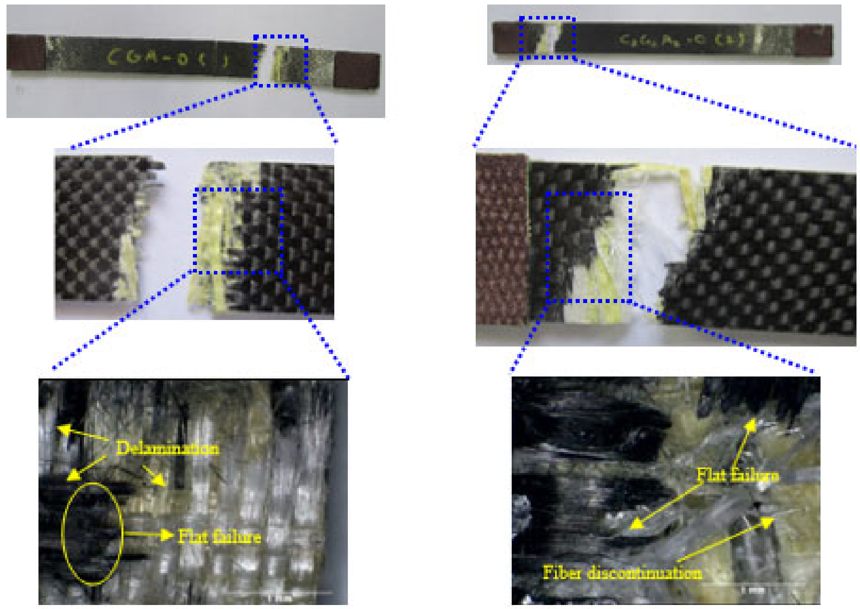

(d) **(CGA)$_4$ at 0/90°** **(e)** **(C$_2$G$_2$A$_2$)$_2$ at 0/90°**

Fig. 10. Composite fracture mode during tensile testing at 0/90° for various stacking sequence

It is observed from the Fig. 9, carbon fiber reinforced composite shows the highest tensile strength among all the stacking sequences so it is required to examine fracture mode at different orientations. Further, it can be also observed that next to the maximum tensile strength was achieved in stacking sequence (CGA)$_4$ which is hybrid composite laminate so fracture mode of this stacking sequence is also required to examine at different orientations.

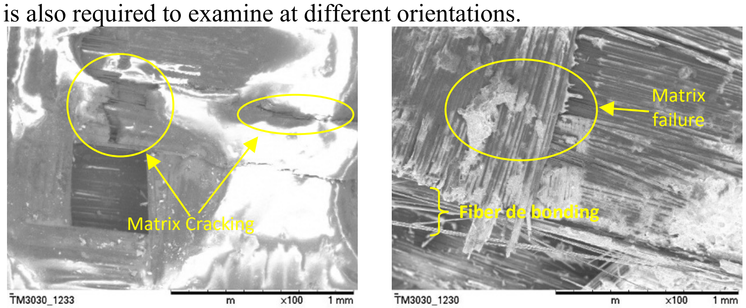

(a) **C-12 at 0/90°** **(b)** **C-12 at 15/75°**

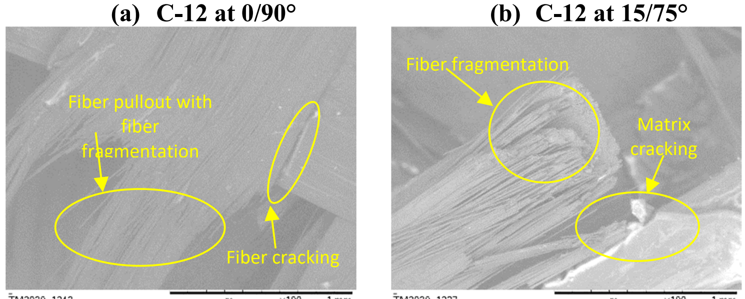

(c) **C-12 at 30/60°** **(d)** **C-12 at 45/-45°**

Fig. 11. Micrographs of stacking sequence C-12 at different orientations

Fig. 11 shows the micrographs of various modes of fracture of carbon reinforced composite laminates at different orientations obtained using Hitachi make Scanning Electron Microscope (SEM). Fig. 11 (a) shows fracture for 0/90 orientation for fully carbon reinforced composite. In this case, it can be seen that tensile failure occurs in loading direction which results in the flat fracture of the reinforcement material. The fiber and matrix cracking can also be seen in the loading direction. Fig. 11 (b) shows the orientation 15/75°, in which fiber fragmentation and matrix fracture can be observed. Crack initiation in fiber through the matrix material for 30/60° orientation is observed in Fig. 11 (c). Fiber pullout with fiber fragmentation can also be seen in this case. Fig. 11 (d) shows the 45/-45° orientation in which matrix fracture and fiber breakage are observed. Fiber pullout of fibers can be seen in a specimen in which fabric is aligned at 45°.

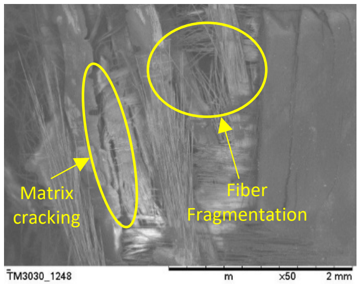

(a) $(CGA)_4$ at 0/90°

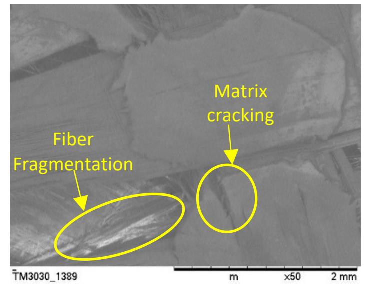

(b) $(CGA)_4$ at 15/75°

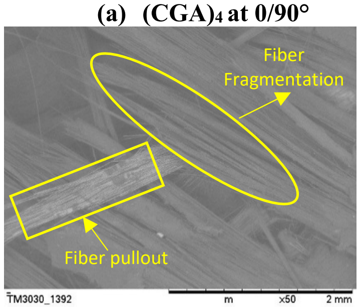

(c) $(CGA)_4$ at 30/60°

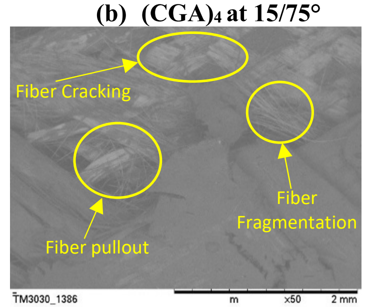

(d) $(CGA)_4$ at 45/-45°

Fig. 12. Micrographs of stacking sequence $(CGA)_4$ at different orientations

Fig. 12 illustrates the SEM images for (CGA)4stacking sequence for all orientations. Fig. 12 (a) shows the (CGA)4at the orientation of 0/90°. The first layer of carbon reinforcement can beseen as fractured with matrix cracking and the next layer of glassreinforcement can be observed with fiber fragmentation. Similarly, in Fig. 12(b), it can also be observed that matrix cracking in the top reinforcementlayer initiates a crack in the specimen. Fig. 12 (c) shows the 30/60°orientation in which fiber fragmentation can be seen in the top layer of thereinforcement and fiber pullout can be observed in subsequent reinforcementlayers. Fig. 12 (d) illustrates the (CGA)4 at 45/-45° through whichit can be observed initial fiber cracking due to tensile loading because ofthis action cracking in fibers turn out into fiber fragmentation. It can alsobe noticed that the next layer of reinforcement is getting pulled out. Fromthis Fig. 12 (d) of the hybrid specimen, it can observe the sequence offracture as the orientation changes. It can be observed that the initial stagespecimen of failure is the matrix cracking due to the tensile loading. Further,Fibers fractured and fragmented in a flat manner but as the orientationincreases fiber pullout can also be observed in the specimen.

3.1.2 Influence of fiber orientation on Tensile strength

In polymer matrix composite, the reinforcement material which is the fibers that has considerable influence on the tensile strength of the composite laminates.

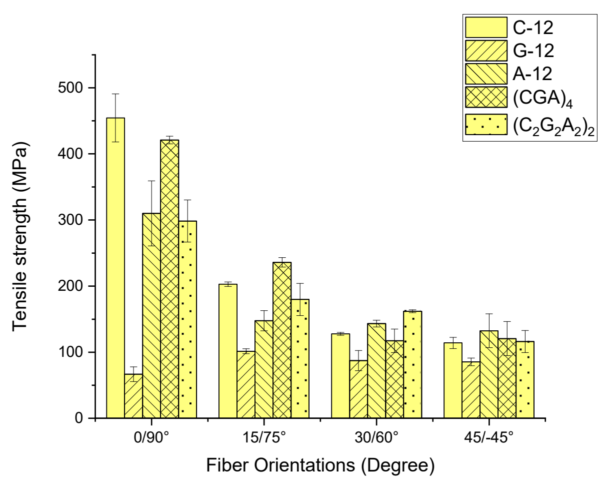

Fig. 13. Tensile strength vs Fiber orientations

Fig. 13 shows the effect of orientation, in combination with stacking sequences on tensile strength. When the fiber orientation was not in line with the loading direction low tensile strength was observed. It was observed that the tensile strength reduced was found with an increase in the fiber orientation. With the increment in orientation pulling force which is acting on fiber laminate. The force is divided into two components in weft and warp direction. Thus low tensile strength was obtained in 45/-45° orientation compared to 0/90°. Further, during increment of orientation notable fiber pullout can be seen at orientation 45/-45° while no fiber pullout can be seen at orientation of 0/90°.

From Fig. 13, it can be noticed that maximum tensile strength was achieved in all stacking sequences at 0/90° orientation compared to other orientation. Hence, it is required to inspect its mode of fracture in different stacking sequences.

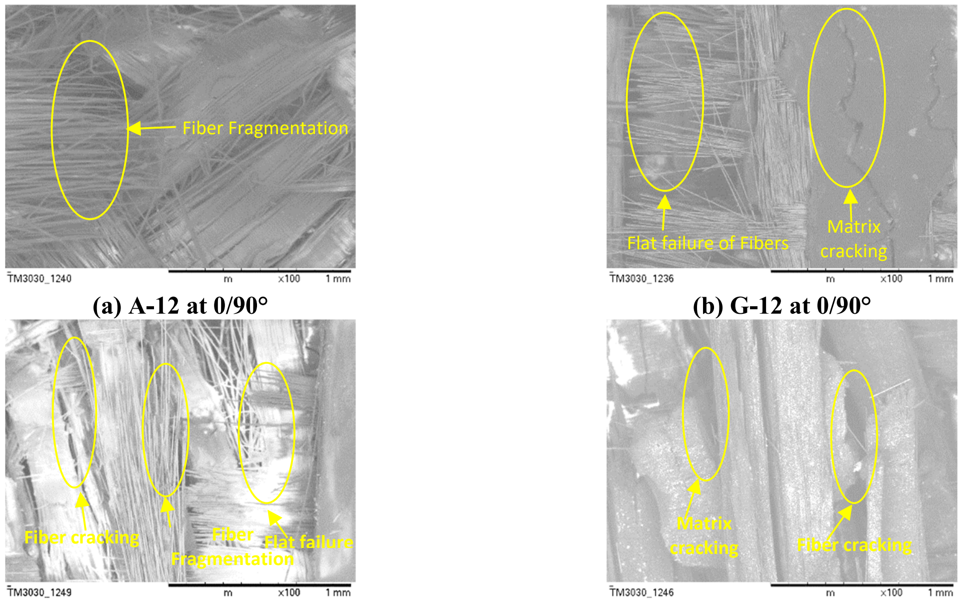

(a) A-12 at 0/90° **(b) G-12 at 0/90°**

(c) $(CGA)_4$ at 0/90° **(d) $(C_2G_2A_2)_2$ at 0/90°**

Fig. 14. Micrographs of different stacking sequence at 0/90° orientations

Fig. 14 shows SEM images for different stacking sequences at 0/90° orientation. Fig. 14 (a) shows the sequence Aramid reinforced composite which consists of 12 plies of aramid. As Aramid fibers have lints so during the fracture, fiber fragmentation in a random manner can be observed with a flat fracture. It is also noticed from Fig. 14 (b) that matrix cracking and fine fiber fragmentation in warp direction occurs in tensile loading direction in glass fiber reinforced composite. Fig. 14 (c) indicates hybrid composite $(CGA)_4$ in this case flat failure of carbon fibers was observed and an adjacent layer which is glass fiber can be seen due to failure of the upper layer. It is also observed that at the initial stage fragmentation the fibers occur during the testing which can result in delamination of the composite laminates. Fig. 14 (d) shows hybrid composite laminate $(C_2G_2A_2)_2$, the matrix cracking and fiber fracture can be observed in this stacking sequence. It is also noticed that the bundle of fibers is separated by a cracking matrix.

3.2 Flexural behavior

Flexural tests measure the mechanical properties of composite samples when subjected to bending loads. Load a flat rectangular sample at three points. The load causes the specimen to bend, creating compressive strain on the upper side, tensile strain on the lower side, and shearing along the mid-plane.

3.2.1 Influence of stacking sequence on flexural strength

Table 3 shows the testing results of the flexural testing. Fig. 15 shows the graph of flexural strength against stacking sequence. From Fig. 15 and Table-3, it is noted that hybrid polymer matrix composite $(C_2G_2A_2)_2$ has maximum flexural strength and glass reinforced composite has the lowest flexural strength. In stacking sequence $(C_2G_2A_2)_2$ two carbon layers were placed in the outermost position, as well as two were in the mid position of the specimen. This arrangement of reinforcements provides better bending strength to the laminate as Carbon fiber exhibits higher bending strength eventually providing higher strength to the entire structure. From the testing results, it is observed that the position of carbon fiber fabric was normal to the bending force which absorbed maximum force exerted by the punch of the flexural bending setup so the high flexural strength was achieved. It is also found that the placement of carbon fiber fabric in the stacking sequence plays an important role. Researcher has reported that during flexural testing that placement of carbon fiber on compression side gives high flexural strength (Subagia and Kim (2013); Park and Jang (1999). The specimen having carbon fiber towards the compression side resists more compressive force than other laminates so increase in flexural strength can be achieved.

Additionally, we have also observed that in both variations of hybrid laminates viz. $(CGA)_4$ and $(C_2G_2A_2)_2$ flexural strength was increased due to the carbon fiber placement on the compression side.

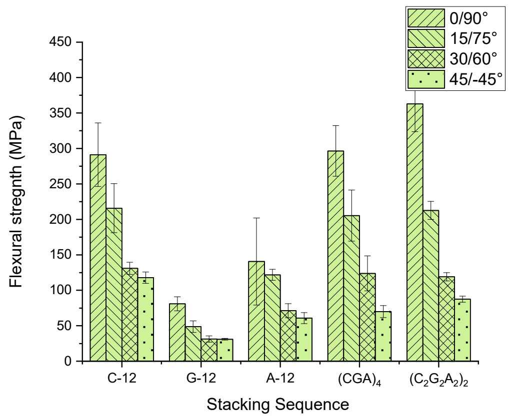

Fig. 15. Flexural strength vs stacking sequence

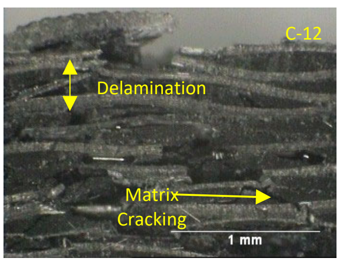

(a) C-12 at 0/90°

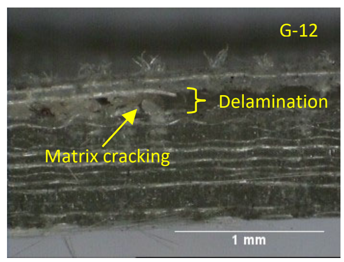

(b) G-12 at 0/90°

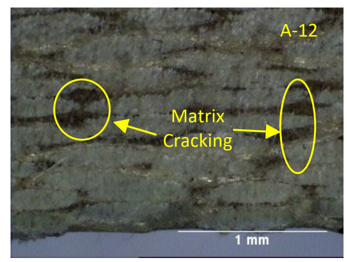

(c) A-12 at 0/90°

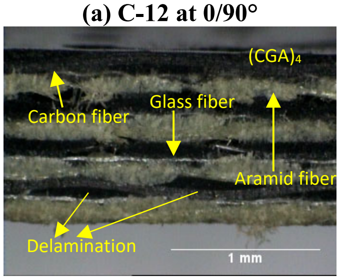

(d) $(CGA)_4$ at 0/90°

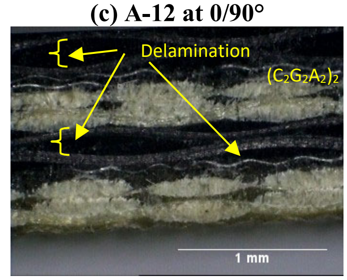

(a) $(C_2G_2A_2)_2$ at 0/90°

Fig. 16. Composite fracture during flexural testing at 0/90° for various stacking sequence

Fig. 16 shows the composite fracture during the flexural test for all five stacking sequences and at 0/90° orientation. From Fig. 16 (a) matrix cracking and fiber delamination of the laminates can be observed in the carbon reinforced composite. Due to compression loading layer by layer crack initiation produces the delamination in the specimen. Fig. 16 (b) shows the glass fiber reinforced laminate in which it can be seen that matrix cracking is initiated and which results in delamination of the outer layer of the specimen. The nature of matrix cracking is found to be brittle. Fig. 16 (c) illustrates the aramid fiber reinforced composites. Where delamination and matrix cracking were difficult to observe because of lint but delamination between layers can be seen. Fig. 16 (d) and (e) respectively show both hybrid laminates viz. $(CGA)_4$ and $(C_2G_2A_2)_2$ where no major matrix cracks were found but delamination of the fibers was observed.

3.2.2 Influence of fiber orientation on Flexural strength

Fiber orientation is an important aspect that influences the flexural behavior of the fiber reinforced composites. Fig. 17 illustrates the graph of flexural strength versus fiber orientations. The orientation 0/90° has the highest flexural strength among all the orientations. The stacking sequence $(C_2G_2A_2)_2$ with 0/90° orientation shows the highest flexural strength while G12 with 45/-45° results in the lowest flexural strength. The orientation 0/90° criss cross structure of plain weave fabric is similar to the net structure. In this kind of structure fibers in the weft and warp direction bear equal compressive load in both directions. While in other orientations load-bearing capacity differs as the orientations increase 0/90° to 45/-45°. As the orientation increases, the flexural strength of the laminate decreases. The reason behind this change was the contact between roller and upper fiber laminate is decreased as fiber orientation increases. During flexural testing of 0/90° laminates, the compression loading direction was aligned with either weft or warp direction which resulted in better contact products. This contact between upper fiber laminate and roller was almost normal to the specimens due to this highest flexural strength was achieved.

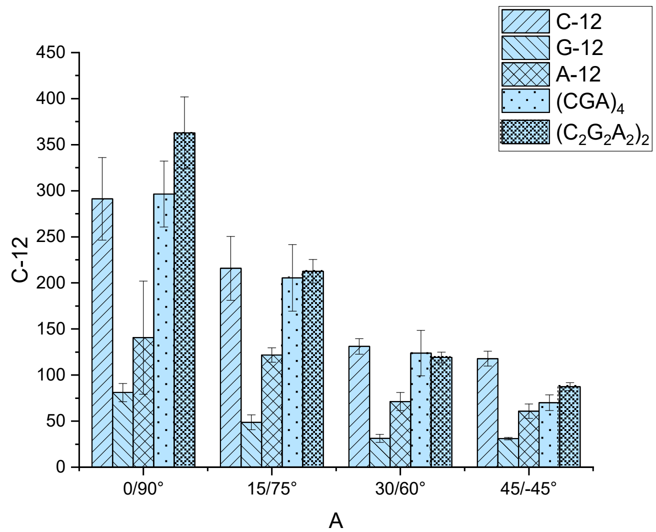

Fig. 17. Flexural strength vs fiber orientations

From the above observations, it can be observed that $(C_2G_2A_2)_2$ stacking sequence at 0/90° has maximum flexural strength. Hence it is required to inspect its mode of fracture at different orientations.

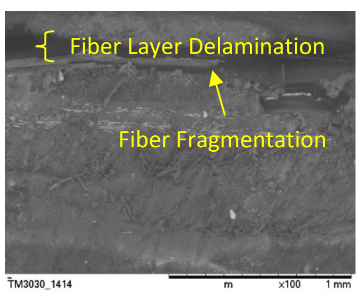

(a) $(C_2G_2A_2)_2$ **at 0/90°**

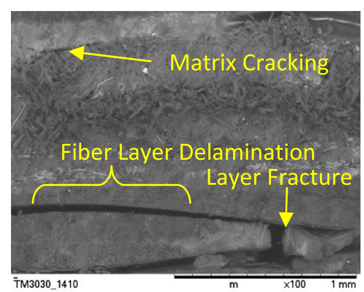

(b) $(C_2G_2A_2)_2$ **at 15/75°**

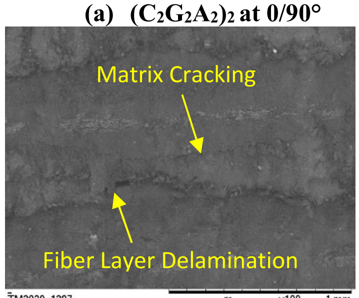

(c) $(C_2G_2A_2)_2$ **at 30/60°**

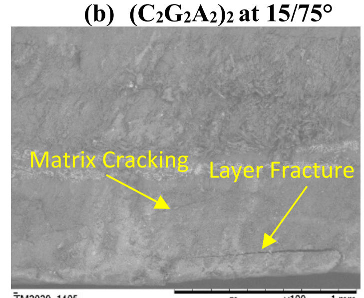

(d) $(C_2G_2A_2)_2$ **at 45/-45°**

Fig. 18. SEM images for $(C_2G_2A_2)_2$ stacking sequence at various orientations

The composite laminates were tested on Shimadzu AG-IS with its compatible flexural testing attachment and software interface. The specimen was rested in a horizontal position over the support length and bending force was exerted by the roller. In composite laminates fracture occurs in the fiber layer along the bending force direction. These fractures could be initiated by micro cracking in the matrix which leads to fiber layer delamination and layer fracture. During the testing as these fractures occur in specimens, the roller retracts the bending force. Hence it is required to examine the specimen under a Scanning Electron Microscope to visualize the mode of fracture in the specimen. Fig. 18 shows the micro images of $(C_2G_2A_2)_2$ stacking sequence at various orientations. Fig. 18 (a) shows fiber layer delamination and fiber fragmentation in bending force direction which leads to failure of other layers of the specimen. From Fig. 18 (b), Matrix cracking and fiber delamination can be observed. It was also observed that as the fiber delamination progresses fiber failure occurs. Fig. 18 (c) illustrates matrix cracking between two reinforcements and which leads to fiber layer delamination. From Fig. 18 (d) matrix cracking and fiber layer fracture can be observed in the specimen.

4. Conclusions

In the present research, composite sheets were manufactured with VARTM process with various stacking sequences and fiber orientations. It was observed that tensile strength and flexural strength was influenced by the fiber orientation and stacking sequence of the reinforcements. The pattern of fracture in various stacking sequences and fiber orientations were explained using SEM micrographs. From the current research following conclusions could be drawn:

1. Higher tensile strength is achieved in Carbon-reinforced composite compared to other stacking sequences. It can also be seen that hybridization of carbon fiber fabric with other fabric results in better tensile strength.
2. Fiber orientation and loading direction during tensile testing play a vital role in the mode of fracture. If both are aligned in the same direction, specimen fracture can be observed in only warp direction which shows a flat fracture. If both are not in the same direction fiber pullout is observed depending on the fiber orientation.
3. The outside layer of carbon fiber fabric results in maximum flexural strength in the hybrid composite laminates with $(C_2G_2A_2)_2$ stacking sequence.
4. 0/90° plain weave structure bears more compressive load during the flexural testing of composite laminates. The orientation is a contributing parameter for the composite manufacturing processes.
5. As the fiber orientation increases, tensile and flexural strength decreases.

Declaration of Conflicting Interests

The authors declare that they have no conflict of interest.

Funding

The authors received no financial support for the research, authorship, and/or publication of this article.

References

ASTM Committee D-30 on Composite Materials. (2008). *Standard test method for tensile properties of polymer matrix composite materials*. ASTM international.

ASTM International. (2015). *Standard test method for flexural properties of polymer matrix composite materials*. ASTM International.

Balaji, A., Sivaramakrishnan, K., Karthikeyan, B., Purushothaman, R., Swaminathan, J., Kannan, S., & Madieen, A. H. (2019). Study on mechanical and morphological properties of sisal/banana/coir fiber-reinforced hybrid polymer composites. *Journal of the Brazilian Society of Mechanical Sciences and Engineering*, *41*(9), 1-10.

Bhagat, V. K., Biswas, S., & Dehury, J. (2014). Physical, mechanical, and water absorption behavior of coir/glass fiber reinforced epoxy based hybrid composites. *Polymer Composites*, *35*(5), 925-930.

Bhudolia, S. K., Kam, K. K., & Joshi, S. C. (2018). Mechanical and vibration response of insulated hybrid composites. *Journal of Industrial Textiles*, *47*(8), 1887-1907.

Bindal, A., Singh, S., Batra, N. K., & Khanna, R. (2013). Development of glass/jute fibers reinforced polyester composite. *Indian Journal of Materials Science*, *2013*.

Deng, C., Jiang, J., Liu, F., Fang, L., Wang, J., Li, D., & Wu, J. (2015). Effects of electrophoretically deposited graphene oxide coatings on interfacial properties of carbon fiber composite. *Journal of materials science*, *50*(17), 5886-5892.

Dippenaar, D. J., & Schreve, K. (2013). 3D printed tooling for vacuum-assisted resin transfer moulding. *The International Journal of Advanced Manufacturing Technology*, *64*(5), 755-767.

Dong, C., & Davies, I. J. (2012). Optimal design for the flexural behaviour of glass and carbon fibre reinforced polymer hybrid composites. *Materials & Design*, *37*, 450-457.

Flynn, J., Amiri, A., & Ulven, C. (2016). Hybridized carbon and flax fiber composites for tailored performance. *Materials & Design*, *102*, 21-29.

Golzar, M., & Poorzeinolabedin, M. (2010). Prototype fabrication of a composite automobile body based on integrated structure. *The International Journal of Advanced Manufacturing Technology*, *49*(9-12), 1037-1045.

Islam, M. S., Melendez-Soto, E., Castellanos, A. G., & Prabhakar, P. (2015). Investigation of woven composites as potential cryogenic tank materials. *Cryogenics*, *72*, 82-89.

Kaushik, P., Jaivir, J., & Mittal, K. (2017). Analysis of mechanical properties of jute fiber strengthened epoxy/polyester composites. *Engineering Solid Mechanics*, *5*(2), 103-112.

Murugan, R., Ramesh, R., Padmanabhan, K., Jeyaraam, R., & Krishna, S. (2014). Experimental investigation on static mechanical properties of glass/carbon hybrid woven fabric composite laminates. In *Advanced Materials Research* (Vol. 903, pp. 96-101). Trans Tech Publications Ltd.

Naik, N. K., Sirisha, M., & Inani, A. (2014). Permeability characterization of polymer matrix composites by RTM/VARTM. *Progress in aerospace sciences*, *65*, 22-40.

Olodo, E., Adanhounme, V., Adjovi, E., & Shambina, S. (2014). Experimental study of a woven fiberglass composite delamination under impact shock. *Engineering Solid Mechanics*, *2*(3), 163-172.

Park, R., & Jang, J. (1999). Performance improvement of carbon fiber/polyethylene fiber hybrid composites. *Journal of materials science*, *34*(12), 2903-2910.

Selver, E., Ucar, N., & Gulmez, T. (2018). Effect of stacking sequence on tensile, flexural and thermomechanical properties of hybrid flax/glass and jute/glass thermoset composites. *Journal of Industrial Textiles*, *48*(2), 494-520.

Sezgin, H., & Berkalp, O. B. (2017). The effect of hybridization on significant characteristics of jute/glass and jute/carbon-reinforced composites. *Journal of Industrial Textiles*, *47*(3), 283-296.

Simacek, P., Eksik, Ö., Heider, D., Gillespie Jr, J. W., & Advani, S. (2012). Experimental validation of post-filling flow in vacuum assisted resin transfer molding processes. *Composites Part A: Applied Science and Manufacturing*, *43*(3), 370-380.

Singh, J., Kumar, M., Kumar, S., & Mohapatra, S. K. (2017). Properties of glass-fiber hybrid composites: a review. *Polymer-Plastics Technology and Engineering*, *56*(5), 455-469.

Song, J. H. (2014). Manufacturing method of carbon and glass fabric composites with dispersed nanofibers using vacuum-assisted resin transfer molding. *e-Polymers*, *14*(5), 345-352.

Song, J. H. (2016). Tensile and bending behavior for woven carbon-aramid/epoxy hybrid composites with various lamination structures by the VARTM method. *Fibers and Polymers*, *17*(8), 1269-1276.

Subagia, I. A., & Kim, Y. (2013). A study on flexural properties of carbon-basalt/epoxy hybrid composites. *Journal of Mechanical Science and Technology*, *27*(4), 987-992.

Swolfs, Y., Verpoest, I., & Gorbatikh, L. (2019). Recent advances in fibre-hybrid composites: materials selection, opportunities and applications. *International Materials Reviews*, *64*(4), 181-215.

Teixeira, T. A., & Souza, J. A. (2019). Computational modeling of resin infusion process applied to small vessel hulls. *Journal of the Brazilian Society of Mechanical Sciences and Engineering*, *41*(10), 1-9.

Umer, R., Li, Y., Dong, Y., Haroosh, H. J., & Liao, K. (2015). The effect of graphene oxide (GO) nanoparticles on the processing of epoxy/glass fiber composites using resin infusion. *The International Journal of Advanced Manufacturing Technology*, *81*(9), 2183-2192.